Hindawi
Mathematical Problems in Engineering
Volume 2022, Article ID 6744349, 11 pages
https://doi.org/10.1155/2022/6744349

Research Article

Chaotic Oscillations in a Fractional-Order Circuit with a Josephson Junction Resonator and Its Synchronization Using Fuzzy Sliding Mode Control

Balamurali Ramakrishnan,[1] Murat Erhan Cimen,[2] Akif Akgul ,[3] Chunbiao Li ,[4,5] Karthikeyan Rajagopal,[1] and Hakan Kor[3]

[1]*Center for Nonlinear Systems, Chennai Institute of Technology, Chennai, India*
[2]*Sakarya University of Applied Sciences, Faculty of Technology, Department of Electrical and Electronics Engineering, Sakarya 54050, Turkey*
[3]*Hitit University, Faculty of Engineering, Department of Computer Engineering, Corum 19030, Turkey*
[4]*Jiangsu Collaborative Innovation Center of Atmospheric Environment and Equipment Technology (CICAEET), Nanjing University of Information Science & Technology, Nanjing 210044, China*
[5]*Jiangsu Key Laboratory of Meteorological Observation and Information Processing, Nanjing University of Information Science & Technology, Nanjing, China*

Correspondence should be addressed to Akif Akgul; akifakgul@hitit.edu.tr

Received 2 June 2022; Accepted 20 July 2022; Published 28 August 2022

Academic Editor: Abdellatif Ben Makhlouf

Copyright © 2022 Balamurali Ramakrishnan et al. This is an open access article distributed under the Creative Commons Attribution License, which permits unrestricted use, distribution, and reproduction in any medium, provided the original work is properly cited.

A linear resistive capacitive inductive shunted model of a Josephson junction with a topologically nontrivial behaviour is considered in this paper. We have considered a fractional-order flux-controlled memristor to effectively model the feedback flux effects across the Josephson junction (JJ). The mathematical model of the proposed JJ oscillator is derived, and the dimensionless model is used to study the various dynamical properties of the oscillator. The stability plot shows that the proposed oscillator has both stable and unstable regions of oscillations for different choices of equilibrium points and fractional order. The bifurcation plots are presented to understand the route to crisis, and we have also shown that the oscillator has regions of coexisting attractors. We have also achieved the synchronization of the proposed oscillator using fuzzy sliding mode control with the master and slave systems considered with different parameter sets. The chattering amplitude is estimated by using the fuzzy logic, and it is used in the synchronization algorithm to minimize the error.

1. Introduction

The complex nature of nonlinear dynamical systems has long been a problem for science, but as computers have evolved, they have become much better at handling it. Particularly, in some nonlinear systems, chaotic behaviour is unveiled for interesting parameter values. The presence of chaotic behavior is often regarded as undesirable and problematic. The investigation about the sensitivity of the nonlinear dynamical system becomes mandatory for understanding how systems behave during working range of parameters. Even though there are lots of studies conducted on this topic, study of irregular behaviours of the nonlinear dynamical system is a potential research area. Fractional calculus is an effective tool for exploring the unexplored region of system characteristics [1, 2]. Chaotic systems are identified with more intricate response for not only parameter changes but also initial conditions. There are many studies found in analysing the chaotic systems with fractional-order treatment, and really useful results were obtained. On the contrary some literatures proved that not all the chaotic systems need to study with fractional-order. So, it is obvious a question in our mind "which chaotic systems actually needs fractional-order treatment?" During the course of finding the answer for the question, we come up with a better understanding of fractional-order theory. The fractional-order approach is particularly suited for analyzing chaotic systems that exclusively depend on the instant of time but they are affected by the history of the preceding stage [1–4]. Bifurcation theory is a mathematical tool that describes effectively the transformation of behaviour from one state to another [5]. Using this mathematical tool and fractional-order treatment will provide an insight analysis of nonlinear dynamical systems. It is proved that the fractional-order form holds unlimited memory and provides more degrees of freedom [1, 3, 6]. Hence, investigation of chaotic behaviour in nonlinear dynamical systems with fractional-order circuits is more complex and unearthed interesting characteristics.

Fractional systems can be used in chemical processes [7], biological systems [8], electrochemical systems [9], viscoelastic systems [7, 10], and propagation of electromagnetic waves [7, 11]. In the literature, it is encountered in the control of such systems or synchronization applications, communication [12], control of power systems, or control of chemical processes [13, 14]. Many methods such as PID [15], sliding mode control [7], backstepping control [16, 17], fuzzy sliding mode control [18], and adaptive sliding mode control [19] have been used in the control of such systems. The major significance of SMC is that it has a robust structure against varying parameters [7, 20]. Thanks to that, the controller keeps the system on the designed surface under varying conditions. Moreover, the SMC method is a powerful method of controlling high-order systems against disturbances and parameter uncertainties [21, 22]. On the other hand, sliding mode control suffers from high amplitude chattering problem. In this study, fuzzy logic is used to determine the chattering amplitude. In [23], a set of linguistic rules is determined and adaptive SMC control law can be applied for chaotic systems. It has also been studied in the control and synchronization of time-invariant/varying and SMC chaotic systems [23, 24]. In addition, studies have been made on determining the surface of fractional chaotic systems with fuzzy logic [25, 26]. In the study, rather than determining the surface, the chattering amplitude was determined by fuzzy logic and synchronization was achieved with the control rule.

Current-voltage relation can be described with resistor; similarly, the relation between voltage and charge can be described with capacitor; finally, the current-magnetic flux is defined with inductor. Memristor is a novel component, which defines the inter-connection of charge and magnet flux. Our interest in memristor is for its memory effect. From the literature, we identified that the memristor coupling can effectively describe the effects of memory and show the relation between output voltage and magnetic flux by generating induction current [2]. The nonlinearity of electric circuit is engendered, and the dynamical behaviour becomes more complex when memristor is used in circuits because the memductance is dependent on the inputs current [15]. Introduction of memristor in a circuit engendered the nonlinearity and exhibit intricate behaviours, it is because, the dependency of the memductance on the input current.

The application of Josephson junction in superconductors [27–29] is considered as a milestone since its discovery in the 1960s and attracts attention due to its significance and suitability for different circuits. These devices are very high speed and sensitivity [30]. The prominence is now extended to various applications such as analog devices [31]. Many studies [32–36] discussed the usage of Josephson junction for high-frequency oscillators with high critical current density, but most of them are deliberately designed to avoid chaotic regions. Initial investigations show the need of rigorous studies to establish this application. An asymmetric memristive diode-bridge-based jerk circuit is proposed in [37] and studied the asymmetric coexisting bifurcations, and it has a potential future works to new applications.

Motivated from the above discussion, we propose a novel chaotic circuit consisting both memristor and Josephson junction, and dynamical behaviours are analysed using the fractional-order approach. Section 2 deals the formulation of circuit and its mathematical model. Section 3 provides the numerical simulations. Section 4 describes synchronization with fuzzy sliding mode. Section 5 presents the simulation results. Finally, we highlight the significance and effectiveness of the proposed system in conclusion.

2. Mathematical Model

A Josephson junction with topologically nontrivial barrier can be defined with a linear resistive capacitive inductive shunted model discussed in [3, 38, 39]. We include a memristor parallel to the Josephson junction to derive the new proposed chaotic oscillator consisting of both memristor and Josephson junction as discussed in [40], where the authors considered a flux-controlled memristor with a Josephson junction [3]. This memristor is included to model the feedback flux effects in a Josephson junction device. We propose the new chaotic oscillator as shown in Figure 1 wherein we used a fractional-order memristor whose mathematical model is used from [2].

The circuit of Figure 1 is made of a flux-controlled fractional-order memristor W, a Josephson junction with topologically nontrivial barrier J, a capacitor C, and a shunt inductor L_S whose internal resistance is R_S. By applying an external DC current I, the current passing through and the voltage across the circuit elements can be derived using the KVL and KCL as

$$\begin{aligned} I &= I_J + C\frac{dV}{d\tau} + \frac{V}{R} + I_S + I_W, \\ V &= L_S\frac{dI_S}{d\tau} + R_S L_S, \\ V &= \frac{h}{4e}\frac{d\phi}{d\tau}, \\ I_W &= \frac{d^q\rho(\varphi)}{d\tau^q}, \end{aligned} \tag{1}$$

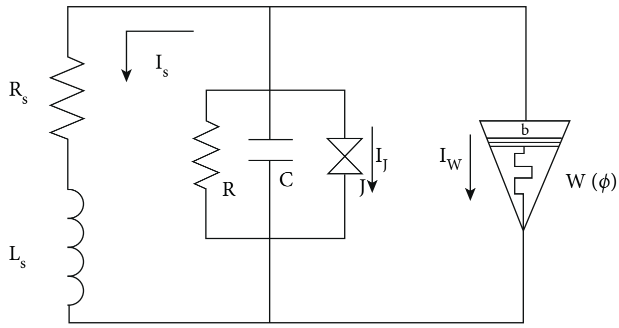

FIGURE 1: Fractional-order memristor: Josephson junction circuit.

where h is the Planck constant, e is the charge of the electron, and q is the fractional order of the memristor. The memductance function can be derived with Faraday's law through which we can define the electromagnetic induction current as

$$I_W = \frac{d^q \rho(\varphi)}{d\tau^q} = \frac{d^q \rho(\varphi)}{d\varphi^q} \frac{d^q \varphi}{d\tau^q}, \tag{2}$$

whose memductance is given by

$$W(\varphi) = \frac{d^q q(\varphi)}{d\varphi^q} = \alpha + 3\beta\varphi^2. \tag{3}$$

Using (3) in (2),

$$I_M = \frac{d^q q(\varphi)}{d\varphi^q} \frac{d^q \varphi}{d\tau^q} = k_0 W(\varphi) V. \tag{4}$$

By using equations (3) and (4) in equation (1) and by substituting dimensionless state variables and parameters, we can derive the mathematical model as

$$\begin{aligned}
\frac{d^{q_v} v}{dt} &= \frac{1}{\beta_C}\left(I_{DC} - i_S - \beta_C v - \sin(\phi) - m\sin(\phi) - k_0 W(\varphi) v\right), \\
\frac{d^{q_{i_s}} i_S}{dt} &= \frac{1}{\beta_L}(v - i_S), \\
\frac{d^{q_\phi} \phi}{dt} &= v, \\
\frac{d^{q_\varphi} \varphi}{dt^q} &= k_1 v - k_2 \varphi,
\end{aligned} \tag{5}$$

where the dimensionless state variables are defined as $v = V/R_S I_C, i_S = I_S/I_C, t = \tau\omega_0$ and the dimensionless parameters are $\beta_C = \mathrm{ECI}_J R_S^2/h, \beta_R = R_S^2 I_J/R, \beta_L = E L_S I_J/h$, $I_{DC} = I/I_J, \omega_0 = E R_S I_J/h, E = 2\pi e$. The fractional orders of the system are $q = [q_v; q_{i_s}; q_\phi; q_\varphi]$.

To numerically simulate system (5), we considered the modified Adams–Bashforth method [41] for the Caputo–Fabrizio (CF) fractional operator [6]. By definition, the general form of a CF fractional operator can be described in the form

$$\begin{aligned}
{}_0^{CF}D_t^q \varphi(t) &= F(t, X(t)), \\
\varphi(0) &= \varphi_0.
\end{aligned} \tag{6}$$

The definition in (6) can be modified as

$$\frac{M(q)}{1-q} \int_0^t X^1(\tau) \exp\left(-q\frac{t-\tau}{1-q}\right) d\tau = F(t, X). \tag{7}$$

By the definition from [41], (6) can be numerically expanded to the form

$$\begin{aligned}
X(n+1) - X(n) &= \frac{1-q}{M\Gamma(q)} F(t_n, X_n) - F(t_{n-1}, X_{n-1}) \\
&\quad + \frac{q}{1-q} \int_{t_n}^{t_{n+1}} F(t, X(t)) dt.
\end{aligned} \tag{8}$$

The solution of (8) can be derived as

$$\begin{aligned}
X(n+1) &= X(n) + \left(\frac{(1-q)}{m\Gamma(q)} + \frac{3q\Delta t}{2m(q)}\right) F(t_n, X_n) \\
&\quad - \left(\frac{(1-q)}{m\Gamma(q)} + \frac{q\Delta t}{2m(q)}\right) F(t_{n-1}, X_{n-1}).
\end{aligned} \tag{9}$$

Using (7) in (5), we could derive the solution for the fractional-order system as

$$\begin{aligned}
v(n+1) &= v(n) + \left(\frac{(1-q_v)}{m\Gamma(q_v)} + \frac{3q_v\Delta t}{2m(q_v)}\right) \\
&\quad - \left(\frac{(1-q_v)}{m\Gamma(q_v)} + \frac{q_v\Delta t}{2m(q_v)}\right) \\
i_s(n+1) &= i_s(n) + \left(\frac{(1-q_{i_s})}{m\Gamma(q_{i_s})} + \frac{3q_{i_s}\Delta t}{2m(q_{i_s})}\right)\left(\frac{1}{\beta_c}(v(n) - i_s(n))\right) \\
&\quad - \left(\frac{(1-q_{i_s})}{m\Gamma(q_{i_s})} + \frac{q_{i_s}\Delta t}{2m(q_{i_s})}\right)\left(\frac{1}{\beta_c}(v(n-1) - i_s(n-1))\right), \\
\phi(n+1) &= \phi(n) + \left(\frac{(1-q_\phi)}{m\Gamma(q_\phi)} + \frac{3q_\phi\Delta t}{2m(q_\phi)}\right)(v(n)) \\
&\quad - \left(\frac{(1-q_\phi)}{m\Gamma(q_\phi)} + \frac{q_\phi\Delta t}{2m(q_\phi)}\right)(v(n-1)), \\
\varphi(n+1) &= \varphi(n) + \left(\frac{(1-q_\varphi)}{m\Gamma(q_\varphi)} + \frac{3q_\varphi\Delta t}{2m(q_\varphi)}\right)(k_1 v(n) - k_2\varphi(n)) \\
&\quad - \left(\frac{(1-q_\varphi)}{m\Gamma(q_\varphi)} + \frac{q_\varphi\Delta t}{2m(q_\varphi)}\right)(k_1 v(n-1) - k_2\varphi(n-1)).
\end{aligned} \tag{10}$$

By proper selection of the system parameters and commensurate fractional orders q, the circuit in Figure 1 exhibits chaotic oscillations. The system parameters are defined as $\beta_C = 0.707, \beta_L = 2.5, \beta_R = 0.06, k_1 = 0.1, k_2 = 0.2$; $k_0 = 0.8, \alpha = 0.01, \beta = 0.01, m = 0.6, I_{DC} = 2, q = 0.98$. The initial conditions of the state variables are [0, 0, 1, 0], and the phase portraits are shown in Figure 2 for the fractional order $q = 0.95$.

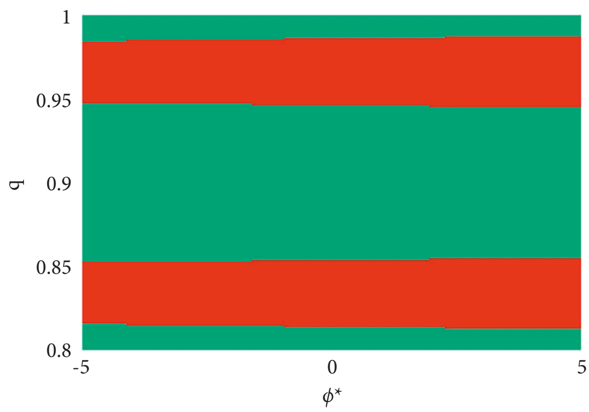

FIGURE 2: The stable and unstable regions shown for various values of ϕ^* and q.

3. Numerical Analysis and Discussion

It can be easily noted that system (5) has infinite equilibrium points which can be calculated by solving $\sin(\phi) + m\sin(\phi) = I_{DC}$ using the Newton–Raphson method. Solving this equation, we could see that the system has no, two, or four roots depending on the value of parameters (I_{DC}, m). Let us assume that the equilibrium points are $[0, 0, \phi^*, 0]$.

Theorem 1. *For system (5) with incommensurate fractional order to be globally asymptotically stable in the Lyapunov sense, the necessary condition can be defined as* $\{arg(\lambda_i)\} > (q\pi/2)$, *where* λ_i *are the roots of characteristic polynomial for each* E_i.

The characteristic polynomial of system (5) for the equilibrium points $[0, 0, \phi^*, 0]$ is given by

$$\lambda^4 + 0.6196\lambda^3 + +. \tag{11}$$

By using the theorem, we could say that the condition for stability is that the fractional order $q < (2/\pi)|\arg(\lambda)|$ for all λ. We have shown the stable and unstable regions in Figure 2 where the stable regions are shown by red colour and unstable regions are shown by pale green.

To investigate the sensitivity of the nonlinear dynamical system with respect to parameter changes, bifurcation diagram is an effective mathematical tool. The influence of parameter changes on the proposed system is analysed in this section. Firstly, we showed the bifurcation diagram for the parameter k_0 variation. The range considered for the investigation is $0 \le k_0 \le 2$. It is observed that system (5) under consideration shows very rich bifurcation structures when slowly tuning the control parameter k_0. From Figure 3(a), we can easily identify some striking bifurcation events including period doubling scenario to chaos, period halving exit to chaos, symmetry boundary, and interior crises.

A small change in parameter value ends up with entirely different system behaviours. The oscillation can be periodic, period doubling, or chaotic. In order to reveal fine changes of oscillations, a tiny window is zoomed with the range of 1.02 to 1.16 and presented in Figure 3. Within this piece of range, we could observe periodic, period doubling, and chaotic regions. Multistability is identified as a significant property in nonlinear dynamics [14–19]. With any abrupt change in the states or parameters, the said multistable system may enter into a new stable situation, which may be entirely different from the desired state. Realizing such properties in dynamical systems and investigating the parameter ranges where multistability occurs is essential and interesting. Dark blue dots are obtained by increasing value of control parameter k_0 from 0 to 2 and red dots are obtained by decreasing the value from 2 to 0 in Figure 3(a). The end value of the states is considered as the initial condition for the consecutive iteration. In Figure 3(b), during parameter range $1.146 \le k_0 \le 1.151$, we can recognize multiperiodic oscillation with blue dots and chaotic oscillation with red dots. Hence, the existence of multistability property is highlighted using the bifurcation plot.

Secondly, we considered the bifurcation parameter as m and other parameters are taken as discussed in the previous section. From Figure 4, periodic oscillations (0.2 to 0.31), period doubling (0.376 to 0.425, 0.62 to 0.65, 0.79 to 0.81, 0.90 to 0.91, and more tiny ranges), period halving (0.322 to 0.375), and cascades of chaotic regions (0.31 to 0.321, 0.376 to 0.39, 0.45 to 0.60, and many more small windows) can be observed. The parameter range considered for the investigation is $0.2 \le m \le 1.2$; with this small variation, the system shows variety of oscillations, and very rapidly, it changes the behaviours. The increment of the parameter shows the increase of amplitude of the oscillations, and the frequency of the occurrence of chaotic regions is reduced. We could also observe multistability property, and it is clearly shown in Figure 4(a).

We increased (or decreased) in tiny steps of parameter m and plotted the local maxima of v. The final state at each iteration of the parameter is considered as the initial state for the next iteration. This strategy is identified as forward (blue plot) and backward (red plot) continuation, and it signifies a simple way to localize the window in which the system advances to multistability. In Figure 4(a), the multistability region is identified and highlighted during $0.322 \le m \le 0.35$ parameter range.

Investigating the influence of order while analysing the fractional-order system is more important. In Figure 4(b), we showed how the system behaves when it is treated with different orders. As we mentioned before, the system is very sensitive in nature. We can observe it even a small change it enters from multiperiodical state to chaotic state. For example, for $q = 0.98$, the system shows chaos, for $q = 0.99$, it is with multiperiodic oscillation, and for $q = 1$ (integer order), it oscillates in chaotic behaviour.

4. Fractional Chaotic System Synchronization with Fuzzy Sliding Mode

In this study, although the two systems to be synchronized are the same in structure, the one that is to be synchronized

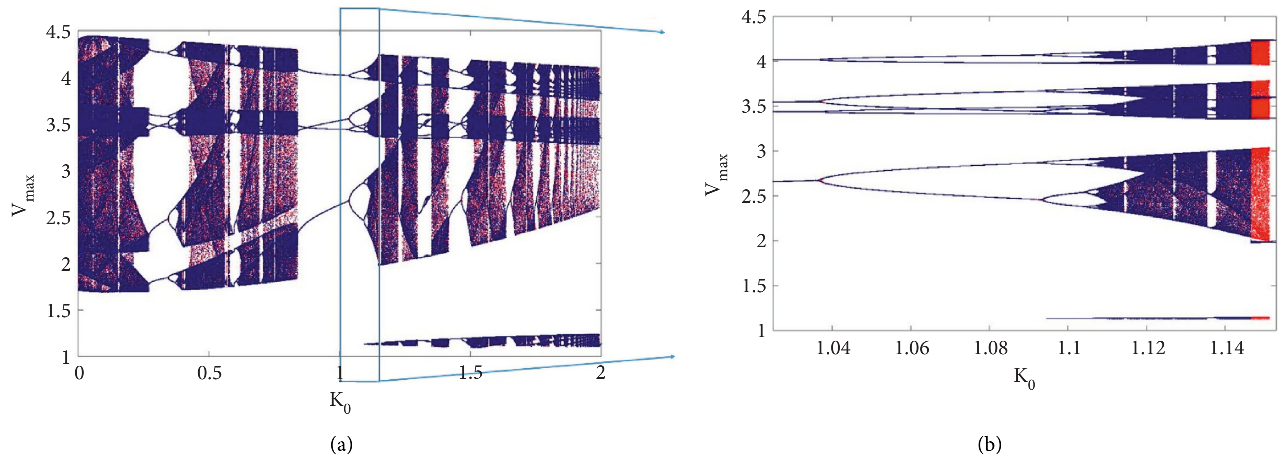

FIGURE 3: (a) Bifurcation diagram of system (5) with varying parameter k_0. (b) The zoomed regions to show coexisting attractors.

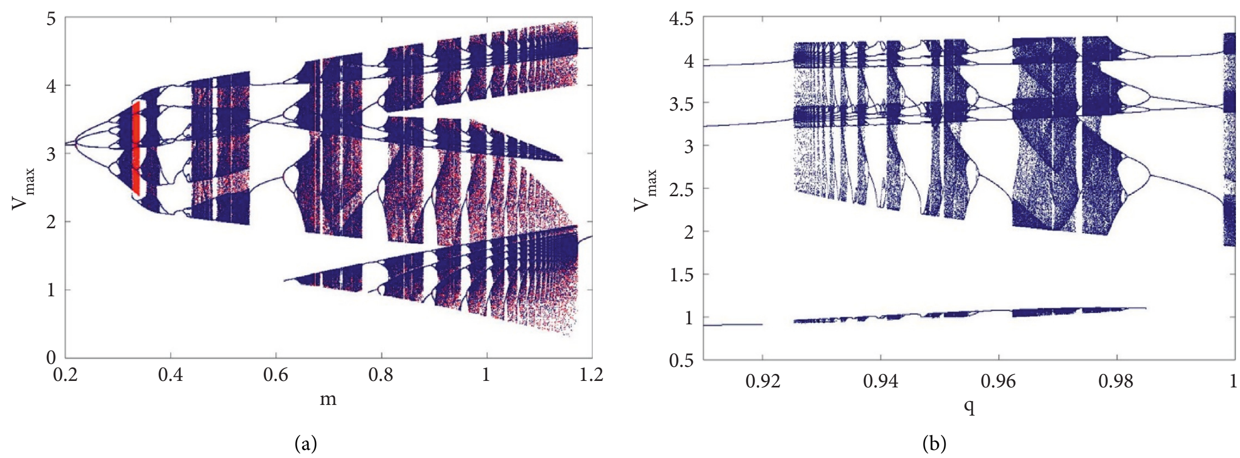

FIGURE 4: (a) Bifurcation diagram of system (5) with varying parameter m. (b) Bifurcation diagram for fractional-order variation for $0.91 \leq q \leq 1$.

parametrically is different. Fractional chaotic system is given in (12) which is parametrically equivalent to (5).

$$\begin{aligned} D^q x_1 &= \frac{1}{\beta_c}\left(I - x_2 - \beta_r x_1 - \sin(x_3)\right. \\ &\quad \left. - m\sin\left(\frac{x_3}{2}\right) - k_0 m_x x_1\right) + u, \\ D^q x_2 &= \frac{1}{\beta_l}(x_2 - x_1), \\ D^q x_3 &= x_1, \\ D^q x_4 &= k_1 x_1 - k_2 x_4. \end{aligned} \tag{12}$$

Fractional chaotic system (12) is given in equation (13) which is to be synchronized to

$$\begin{aligned} D^q y_1 &= \frac{1}{\beta_c}\left(I - y_2 - \beta_r y_1 - \sin(y_3)\right. \\ &\quad \left. - 0.5m\sin\left(\frac{y_3}{2}\right) - k_0 m_x y_1\right), \\ D^q y_2 &= \frac{1}{\beta_l}(y_2 - y_1), \\ D^q y_3 &= y_1, \\ D^q y_4 &= k_1 y_1 - k_2 y_4. \end{aligned} \tag{13}$$

Error dynamics of difference of master and slave system are determined as in (14) to accomplish synchronization.

$$\begin{aligned}
e_1 &= x_1 - y_1,\\
e_2 &= x_2 - y_2,\\
e_3 &= x_3 - y_3,\\
e_4 &= x_4 - y_4,\\
D^q e_1 &= \frac{1}{\beta_c}\begin{pmatrix} I - x_2 - \beta_r x_1 - \sin(x_3) - m\sin\left(\frac{x_3}{2}\right) - k_0 m_x x_1 + u \\ -\left(I - y_2 - \beta_r y_1 - \sin(y_3) - 0.5m\sin\left(\frac{y_3}{2}\right) - k_0 m_x y_1\right)\end{pmatrix},\\
D^q y_2 &= \frac{1}{\beta_l}\left(x_2 - x_1 - (y_2 - y_1)\right),\\
D^q y_3 &= x_1 - y_1,\\
D^q y_4 &= k_1 x_1 - k_2 x_4 - (k_1 y_1 - k_2 y_4).
\end{aligned} \tag{14}$$

4.1. Sliding Mode Control. In order to control a fractional-order system on the sliding surface, it is necessary to define the surface. For this, a surface definition is made as

$$s(t) = k_1 D^{q-1} e_n + k_2 \int_0^t \sum_{i=1}^{n} c_i e_i \mathrm{d}t. \tag{15}$$

Also, this surface function is a derivative as in the following equation:

$$\dot{s}(t) = k_1 D^q e_n + k_2 \sum_{i=1}^{n} c_i e_i = 0. \tag{16}$$

In order to provide stability, the Lyapunov function is determined on the surface defined as in equation (16) and its derivative is taken. Here, the control signal is chosen to ensure $\dot{V} \leq 0$'i in equality (18).

$$V = s^2, \tag{17}$$

$$\dot{V} = s\dot{s}. \tag{18}$$

In this section, the process that is the basis of the sliding mode control will be repeated. In other words, equation (19) must be provided to satisfy $\dot{V} = s\dot{s} \leq 0$. w is a constant value and a required amplitude to satisfy the condition $\dot{V} = s\dot{s} \leq 0$. The corresponding $-\mathrm{sign}(S)$ function will be used. Thus, $\dot{V} \leq s(-\mathrm{sign}(s)) \leq 0$ is obtained. This is given more clearly in Figure 5.

Equations (20) and (21) are obtained by expanding equations (15) and (16).

$$\dot{s}(x) = \begin{cases} w, & \wedge s < 0,\\ -w, & \wedge s \geq 0,\end{cases} \tag{19}$$

$$s(t) = k_1 D^{q-1} e_1 + k_2 \int_0^t (c_1 e_1 + c_2 e_2 + c_2 e_2 + c_2 e_2)\mathrm{d}t, \tag{20}$$

$$\dot{s}(t) = k_1 D^q e_1 + c_1 e_1 + c_2 e_2 + c_2 e_2 + c_2 e_2 = -\mathrm{sign}(s). \tag{21}$$

In equation (21), variables are substituted and expanded as in equation (22). When the equation is arranged to determine the control law to be applied, it is obtained as in the following equation.

$$\begin{aligned}
\dot{s}(t) &= k_1 \frac{1}{\beta_c}\begin{pmatrix} I - x_2 - \beta_r x_1 - \sin(x_3) - m\sin\left(\frac{x_3}{2}\right) - k_0 m_x x_1 \\ -\left(I - y_2 - \beta_r y_1 - \sin(y_3) - 0.5m\sin\left(\frac{y_3}{2}\right) - k_0 m_x y_1\right)\end{pmatrix} + k_1 \frac{u}{\beta_c}\\
&\quad + c_1(x_1 - y_1) + c_2(x_2 - y_2) + c_3(x_3 - y_3) + c_2(x_4 - y_4) = -k_s \mathrm{sign}(s),
\end{aligned} \tag{22}$$

$$u(t) = \frac{\beta_c}{k_1}\begin{bmatrix} -k_1 \frac{1}{\beta_c}\begin{pmatrix} I - x_2 - \beta_r x_1 - \sin(x_3) - m\sin\left(\frac{x_3}{2}\right) - k_0 m_x x_1 \\ -\left(I - y_2 - \beta_r y_1 - \sin(y_3) - 0.5m\sin\left(\frac{y_3}{2}\right) - k_0 m_x y_1\right)\end{pmatrix} \\ -c_1(x_1 - y_1) - c_2(x_2 - y_2) - c_3(x_3 - y_3) - c_4(x_4 - y_4) - k_s \mathrm{sign}(s)\end{bmatrix}. \tag{23}$$

4.2. Fuzzy System. Although fuzzy logic applications are quite easy and have a broad mathematical background, they have an uncomplicated and easy-to-understand structure. Thus, an easier and more durable control law can be produced. Fuzzy logic can be defined with membership functions and rules, which are designed as expert-based and usually expressed linguistically, as well as structures that can learn by data (ANFIS). However, in this study, membership functions and rules, which will be expressed linguistically, have been established. It was then used to determine the amplitude of the control signal using this structure. The general structure of fuzzy logic is given in Figure 6. The basic structure used in the fuzzy logic system is the membership function. Membership functions are used both for fuzzification and for defuzzification. Figure 7 shows the structures of the

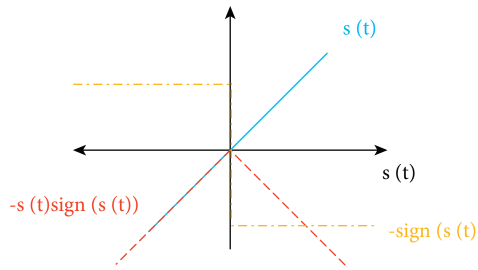

Figure 5: $s(t)$, $-\mathrm{sign}(s(t))$, and $-s(t)\mathrm{sign}(s(t))$ functions.

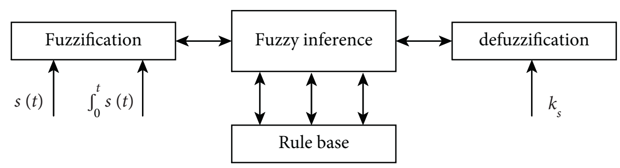

Figure 6: Fuzzy logic inference.

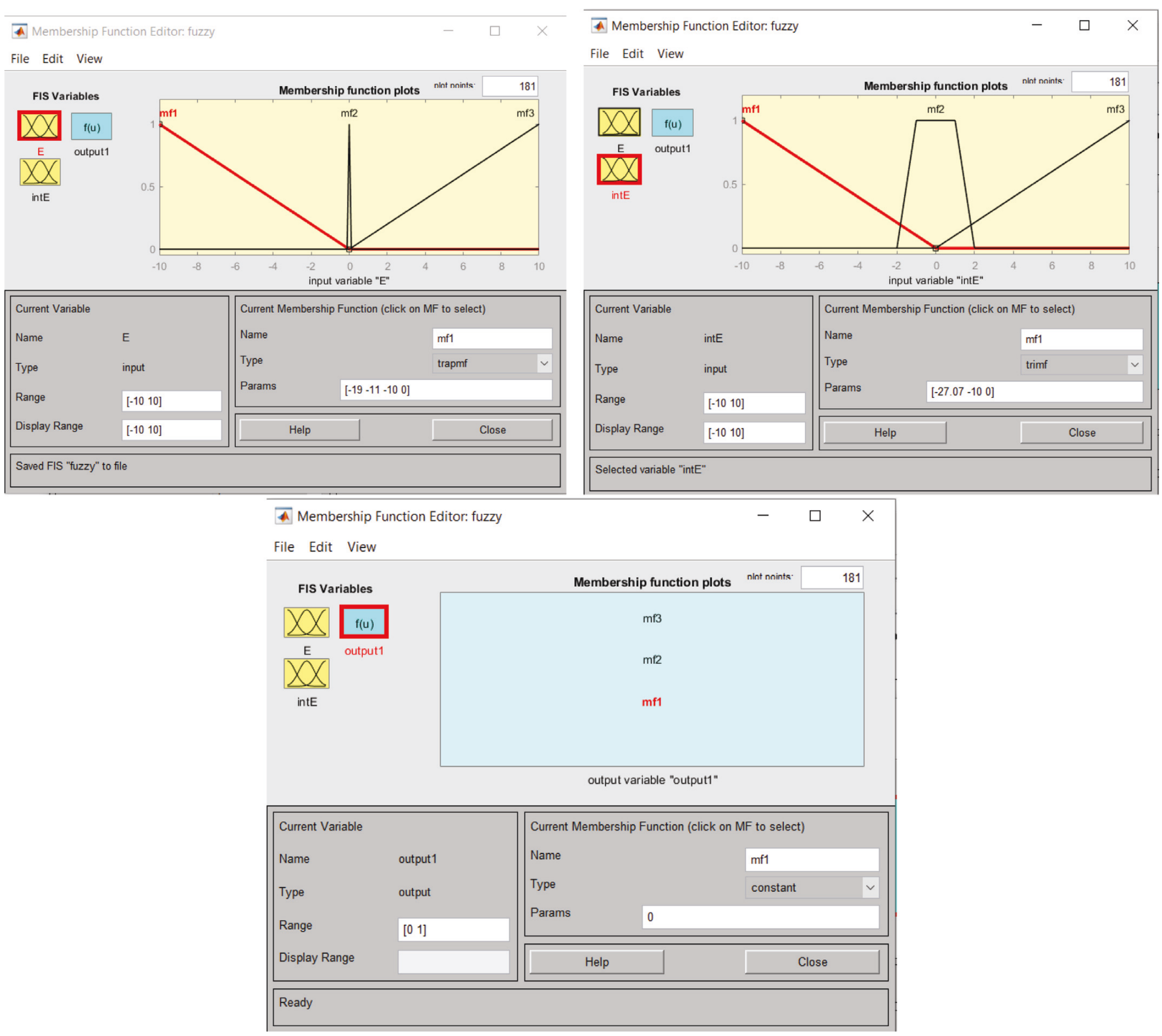

Figure 7: Membership functions used in fuzzy logic.

Table 1: Membership types and values in use in fuzzification and defuzzification.

Input membership function for E		Input membership function for integral E	
MF1	Triangle [−40 −10 0]	1	Triangle [−30 −10 0]
MF2	Triangle [−0.05 0 0.05]	2	Trapeze [−2 −1 1 2]
MF3	Triangle [0 10 20]	3	Triangle [0 10 30]
Output membership function			
MF1	Singleton 0		
MF2	Singleton 20		
MF3	Singleton 5		

Table 2: Rule table for fuzzy inference.

E (integral E)	MF1	MF2	MF3
MF1	MF1	MF1	MF1
MF2	MF1	MF2	MF1
MF3	MF1	MF1	MF1
E/E	MF1	MF3	
MF1	MF3	—	
MF3	—	MF3	
Integral E (integral E)	MF1	MF3	
MF1	MF3	—	
MF3	—	MF3	

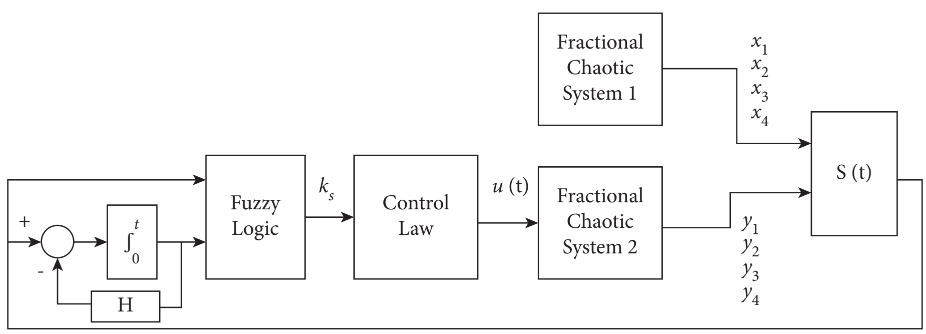

Figure 8: Synchronization of fractional chaotic system by fuzzy sliding mode.

membership functions used in this study, and their information is shown in Table 1. The rule table allowing the association of membership functions for input and output is given in Table 2. A total of 13 rules have been created and these rules are associated with inputs and outputs. This structure used is generally called the Takagi–Sugeno (TS) model in the literature.

Fuzzy logic is used in the modelling and control of systems in decision making and many other situations. In this section, it will be used to adjust the amplitude of the control signal to be applied with the sliding mode control. Fuzzy-based control and sliding mode have been used to prevent rapid and high amplitude changes, which will be applied in the actuator especially in a stationary situation where the error is reduced. The general structure of the system synchronized with fuzzy sliding is given in Figure 8. Especially in the application, when the system approaches the desired surface, the integral value of this error can remain constant. Therefore, a feedback gain (H) is added to reduce the effect of the integral over time, so that this integral value does not remain constant. In order for this structure, which acts as a stable low filter, to be close to the pure integrator, the feedback gain is low.

5. Simulation Studies

The states of the system synchronized in the simulation studies, the amplitude of the control signal, and the amplitude of k_s are given in Figure 9. As can be seen, the system was started to be controlled after 15 seconds and the amplitude of s (t) surface increased until the system was controlled. After the system started to be controlled, $s(t)$ approached 0 and when it reached this value, rapid changes occurred in the control signal at a high frequency due to the amplitude of k_s. However, according to the fuzzy logic decision according to the situation of $s(t)$, the value of k_s was reduced after a certain time and the desired performance was tried to be achieved.

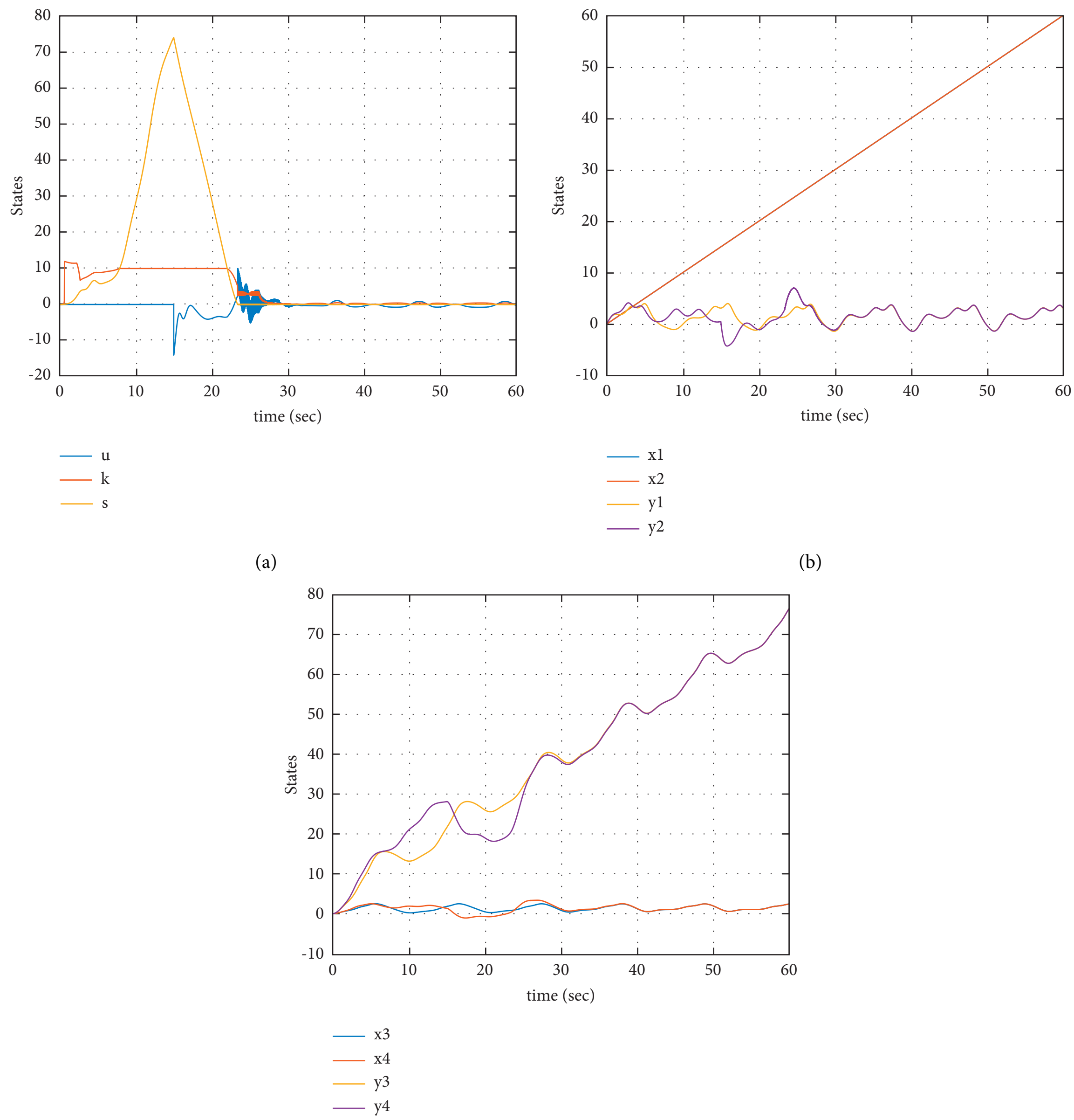

FIGURE 9: States of the (a) synchronized system, (b-c) control signals for $s(t)$ and k_s values.

6. Conclusion

In this study, we have proposed a chaotic oscillator with a Josephson junction device whose feedback flux effects are modelled using a fractional-order memristor. We have derived the dimensionless model of the proposed oscillator and the dynamical properties are investigated using eigenvalues, Lyapunov spectrum, and bifurcation plots. To show the application prospective of the proposed oscillator, we have derived the synchronization between master and slave systems with different parameter sets. The control laws required for the synchronization of the chaotic systems are determined by the sliding mode control technique. Then, fuzzy logic was used to determine the chattering amplitude in the sliding mode control. With the determination of this amplitude, high amplitude changes in the control signal are prevented. Subsequently, this approach has been performed to synchronize fractional chaotic systems. As a future direction, the discussed model can be formulated using the Abu-Shady–Kaabar fractional derivative [42] to obtain analytical solutions and can widen the application in many fields.

Data Availability

The data used to support the findings of this study are included within the article.

Conflicts of Interest

The authors declare that they have no conflicts of interest.

References

[1] I. Podlubny, *Fractional Differential Equations*, Academic Press, San Diego, USA, 1999.

[2] K. Rajagopal, C. Li, F. Nazarimehr, A. Karthikeyan, P. Duraisamy, and S. Jafari, *Chaotic Dynamics of a Simple Wein Bridge Oscillator with Fractional Order Memristor*, Radioengineering, Omaha, Nebraska, USA, 2019.

[3] S. Takougang Kingni, G. Fautso Kuiate, R. Kengne, R. Tchitnga, and P. Woafo, "Analysis of a no equilibrium linear resistive-capacitive-inductance shunted junction model, dynamics, synchronization and application to digital cryptography in its fractional-order form," *Complexity*, vol. 2017, pp. 1–12, Article ID 4107358, 2017.

[4] R. Brown, R. Berezdivin, and L. O. Chua, "Chaos and complexity," *International Journal of Bifurcation and Chaos*, vol. 11, pp. 19–26, 2001.

[5] R. Basiński and Z. Trzaska, "Bifurcations and chaos in dynamical systems," *Elektronika*, vol. 23, no. 2, pp. 7–14, 2008.

[6] M. Caputo and M. Fabrizio, "A new definition of fractional derivative without singular kernel," *Progr. Fract. Differ. Appl.*, vol. 1, pp. 73–85, 2015.

[7] I. Petráš, *Fractional-order Nonlinear Systems: Modeling, Analysis and Simulation*, Springer Science & Business Media, Berlin/Heidelberg, Germany, 2011.

[8] C. Ionescu, A. Lopes, D. Copot, J. T. Machado, and J. Bates, "The role of fractional calculus in modeling biological phenomena: a review," *Communications in Nonlinear Science and Numerical Simulation*, vol. 51, pp. 141–159, 2017.

[9] B. Vinagre and V. Feliu, "Modeling and control of dynamic system using fractional calculus: application to electrochemical processes and flexible structures," *Proc. 41st IEEE Conf. Decision and Control*, vol. 1, no. 1, pp. 214–239, 2002.

[10] H. Abdzadeh-Ziabari and M. G. Shayesteh, "Robust timing and frequency synchronization for OFDM systems," *IEEE Transactions on Vehicular Technology*, vol. 60, no. 8, pp. 3646–3656, 2011.

[11] D. Li, Y. Zhou, C. Zhou, and B. Hu, "Fractional locking of spin-torque oscillator by injected ac current," *Physical Review B*, vol. 83, no. 17, Article ID 174424, 2011.

[12] Q. Li, S. Liu, and Y. Chen, "Combination event-triggered adaptive networked synchronization communication for nonlinear uncertain fractional-order chaotic systems," *Applied Mathematics and Computation*, vol. 333, pp. 521–535, 2018.

[13] K. Rabah and S. Ladaci, "A fractional adaptive sliding mode control configuration for synchronizing disturbed fractional-order chaotic systems," *Circuits, Systems, and Signal Processing*, vol. 39, no. 3, pp. 1244–1264, 2020.

[14] A. S. Balamash, M. Bettayeb, S. Djennoune, U. M. Al-Saggaf, and M. Moinuddin, "Fixed-time terminal synergetic observer for synchronization of fractional-order chaotic systems," *Chaos: An Interdisciplinary Journal of Nonlinear Science*, vol. 30, no. 7, p. 073124, 2020.

[15] K. Rajagopal, L. Guessas, A. Karthikeyan, A. Srinivasan, and G. Adam, "Fractional order memristor no equilibrium chaotic system with its adaptive sliding mode synchronization and genetically optimized fractional order PID synchronization," *Complexity*, vol. 2017, 19 pages, 2017.

[16] P. Prakash, J. P. Singh, and B. Roy, "Fractional-order memristor-based chaotic jerk system with no equilibrium point and its fractional-order backstepping control," *IFAC-PapersOnLine*, vol. 51, no. 1, pp. 1–6, 2018.

[17] M. K. Shukla and B. Sharma, "Stabilization of a class of fractional order chaotic systems via backstepping approach," *Chaos, Solitons & Fractals*, vol. 98, pp. 56–62, 2017.

[18] S. Song, B. Zhang, X. Song, Y. Zhang, Z. Zhang, and W. Li, "Fractional-order adaptive neuro-fuzzy sliding mode H∞ control for fuzzy singularly perturbed systems," *Journal of the Franklin Institute*, vol. 356, no. 10, pp. 5027–5048, 2019.

[19] X.-T. Tran, C. Kwon, and H. Oh, "Adaptive Second-Order Sliding Mode Algorithm-Based Modified Function Projective Synchronization of Uncertain Hyperchaotic Systems," *IEEE Access*, vol. 8, 2020.

[20] T. H. Yan, B. Wu, B. He, W. H. Li, and R. B. Wang, "A novel fuzzy sliding-mode control for discrete-time uncertain system," *Mathematical Problems in Engineering*, vol. 2016, pp. 1–9, 2016.

[21] M. Yahyazadeh, A. Ranjbar Noei, and R. Ghaderi, "Synchronization of chaotic systems with known and unknown parameters using a modified active sliding mode control," *ISA Transactions*, vol. 50, no. 2, pp. 262–267, 2011.

[22] X. Wang, X. Zhang, and C. Ma, "Modified projective synchronization of fractional-order chaotic systems via active sliding mode control," *Nonlinear Dynamics*, vol. 69, no. 1-2, pp. 511–517, 2012.

[23] Y.-J. Niu and X.-Y. Wang, "A novel adaptive fuzzy sliding-mode controller for uncertain chaotic systems," *Nonlinear Dynamics*, vol. 73, no. 3, pp. 1201–1209, 2013.

[24] D. Lin and X. Wang, "Chaos synchronization for a class of nonequivalent systems with restrictive inputs via time-varying sliding mode," *Nonlinear Dynamics*, vol. 66, no. 1-2, pp. 89–97, 2011.

[25] X. Song, S. Song, I. T. Balsera, L. Liu, and L. Zhang, "Synchronization of two fractional-order chaotic systems via nonsingular terminal fuzzy sliding mode control," *Journal of Control Science and Engineering*, vol. 2017, pp. 1–11, 2017.

[26] M. P. Aghababa, "Finite-time chaos control and synchronization of fractional-order nonautonomous chaotic (hyperchaotic) systems using fractional nonsingular terminal sliding mode technique," *Nonlinear Dynamics*, vol. 69, no. 1-2, pp. 247–261, 2012.

[27] T. Uchihashi, "Two-dimensional superconductors with atomic-scale thickness," *Superconductor Science and Technology*, vol. 30, no. 1, Article ID 013002, 2017.

[28] J. Murugan and H. Nastase, "Particle-vortex duality in topological insulators and superconductors," *Journal of High Energy Physics*, vol. 2017, no. 5, pp. 1–12, 2017.

[29] Y. M. Shukrinov, I. R. Rahmonov, K. V. Kulikov et al., "Modeling of LC-shunted intrinsic Josephson junctions in high-Tc superconductors," *Superconductor Science and Technology*, vol. 30, no. 2, Article ID 024006, 2017.

[30] D. Baleanu, Z. B. Guvenc, and J. A. T. Machado, *New Trends in Nanotechnology and Fractional Calculus Applications*, p. 1, Springer, Berlin, Germany, 2010.

[31] D. R. He, W. J. Yeh, and Y. H. Kao, "Transition from quasiperiodicity to chaos in a Josephson-junction analog," *Physical Review B: Condensed Matter*, vol. 30, no. 1, pp. 172–178, 1984.

[32] V. K. Kornev and A. V. Arzumanov, "Josephson-junction oscillation spectral line width for some phase-locked multijunction systems," *Journal de Physique IV*, vol. 8, 1998.

[33] C. B. Whan, C. J. Lobb, and M. G. Forester, "Effect of inductance in externally shunted Josephson tunnel junctrion," *J. Appl. Phys. Rev.*, vol. 77, no. 1, pp. 382–389, 1995.

[34] C. B. Whan and C. J. Lobb, "Complex dynamical behavior in*RCL*-shunted Josephson tunnel junctions," *Physical Review*

E - Statistical Physics, Plasmas, Fluids, and Related Interdisciplinary Topics, vol. 53, no. 1, pp. 405–413, 1996.

[35] A. B. Cawthorne, C. B. Whan, and C. J. Lobb, "Complex dynamics of resistively and inductively shunted Josephson junctions," *Journal of Applied Physics*, vol. 84, no. 2, pp. 1126–1132, 1998.

[36] A. B. Cawthorne, P. Barbara, and C. J. Lobb, "HighFrequency Properties of Two-Dimensional Josephson junction Arrays," *IEEE Transactions on Applied Superconductivity*, vol. 7, no. 2, 1997.

[37] Q. Xu, S. Cheng, Z. Ju, Mo Chen, and H. Wu, "Asymmetric coexisting bifurcations and multi-stability in an asymmetric memristive diode-bridge-based jerk circuit," *Chinese Journal of Physics*, vol. 70, pp. 69–81, 2021.

[38] E. Neumann and A. Pikovsky, "Slow-fast dynamics in Josephson junctions," *The European Physical Journal B (EPJ B) - Condensed Matter*, vol. 34, no. 3, pp. 293–303, 2003.

[39] L. Finger, "On the dynamica of coupled Josephson junction circuits," *International Journal of Bifurcation and Chaos*, vol. 06, no. 07, pp. 1363–1374, 1996.

[40] Ge Zhang, J. Ma, A. Alsaedi, B. Ahmad, and F. Alzahrani, "Dynamical behavior and application in Josephson Junction coupled by memristor," *Applied Mathematics and Computation*, vol. 321, pp. 290–299, 2018.

[41] A. Atangana and E. Bonyah, "Fractional stochastic modeling: new approach to capture more heterogeneity," *Chaos*, vol. 29, no. 1, Article ID 013118, 2019.

[42] M. Abu-Shady and M. K. A. Kaabar, "A generalized definition of the fractional derivative with applications," *Mathematical Problems in Engineering*, vol. 2021, Article ID 9444803, 9 pages, 2021.